Journal of Magnetic Resonance 212 (2011) 26–39

Contents lists available at ScienceDirect

Journal of Magnetic Resonance

journal homepage: www.elsevier.com/locate/jmr

Cardinal series to restore NMR-signals dominated by strong inhomogeneous broadening

Stéphane Rodts *, Dimitri Bytchenkoff *

Université Paris Est, Laboratoire Navier[1] (UMR 8205 ENPC-IFSTTAR-CNRS), 2 allée Kepler, 77420 Champs-sur-Marne, France

ARTICLE INFO

Article history:
Received 6 April 2011
Revised 27 May 2011
Available online 17 June 2011

Keywords:
Cardinal
Bayesian
Interpolation
Extrapolation
Oversampling
Truncation

ABSTRACT

We have devised two numerical methods of restoring incomplete band-limited NMR-signals to integrity by either interpolating or extrapolating them. Both methods are based on use of the finite cardinal series, whose filtering properties were discussed previously, to model signals. They require no prior knowledge about the system under study, but only that the available parts of the signal were oversampled enough. The methods were tested on two types of computer-simulated signal. It proved superior to the linear prediction methods and Lagrange interpolation when applied to signals measured in highly inhomogeneous magnetic fields. The extrapolation method was then applied to restore experimentally-measured refocused FID-signals of a porous medium. The missing parts of the signal of up to several times the size of its Nyquist period could be recovered by either method.

1. Introduction

In most NMR-studies, sampling an analogue signal at regular intervals, whose length is dictated by the signal's band-width, all over the period during which it exists will be conceived as an ideal way of recording data. A linear transformation of a thus acquired data set will result in a spectrum or an image of the studied system. Moreover, some of the samples of the digital signal in the time domain are valuable physical quantities in their own right. The first sample of FIDs, for example, is direct related to the equilibrium magnetisation of various isotopes, which is – according to the Curie law – proportional to the quantity of those isotopes in the chemical compound. Such measurements are also used to monitor the amount of interstitial fluids in porous materials, e.g. water in cements during their settings [1,2] or liquid water in cryometric studies [3,4]. This is also the case of the intensity and/or phase of the summit of echoes measured in CPMG [5,6] or PGSE [7,8] experiments, as they allow to measure spin–spin relaxation rates as well as diffusion and flow propagators in fluids.

There are situations, though, in which only a part of the whole signal is recorded. This can be done deliberately. Thus, the evolution periods in the indirect dimensions were often shortened in the past to speed up lengthy multi-dimensional spectroscopic experiments [9]. Much more efficient methods taking advantage of irregular sampling saw the light of day recently [10–14]. In MRI too, 'partial Fourier imaging' – methods that sample a reduced part of the Fourier space – were shown to allow under certain circumstances to obtain images [15,16].

In some cases, on the other hand, an entire signal cannot be recorded effectively. Recording of the FID-signal normally ought to commence at the moment corresponding to the middle of the last pulse of the pulse sequence, which converts pure or mixed quantum magnetic states of the spin system generated by that time into solely detectable transverse magnetisation. This is, though, effectively impossible when the same coil in the spectrometer's probe is used for both the RF-irradiation of the spins and the detection of the signal those spins induce. Thus the detection can start only after the last RF-pulse has ended or rather a short while after it ended to avoid that intense RF-field generated by the transmitter is fed into the sensitive receiver and burn it. Moreover, in various experiments, a few first samples of the signal produced by the ADC of the spectrometer were sometimes found to have the signal-to-noise ratio several orders of magnitude lower than that of the rest of the data set [17,18], which was presumably brought about by some short-lived transient phenomena in the spectrometer's coil, difficult to compensate for or take into account. This becomes a real problem when studying systems characterised by high intrinsic inhomogeneity of their magnetic susceptibility or/and fast NMR-relaxation, as then a significant initial part of the signal rich in physical, chemical, biological or medical information

* Corresponding authors. Fax: +33 (0)1 40 43 54 50.
E-mail addresses: stephane.rodts@ifsttar.fr (S. Rodts), Dimitri.Bytchenkoff@enpc.fr (D. Bytchenkoff).

[1] The Laboratoire Navier is a civil engineering laboratory associated with the Ecole Nationale des Ponts et Chaussées (ENPC), Institut Français des Sciences et Technologies des Transports, de l'Aménagement et des Réseaux (IFSTTAR) and Centre National pour la Recherche Scientifique (CNRS).

1090-7807/$ - see front matter © 2011 Elsevier Inc. All rights reserved.
doi:10.1016/j.jmr.2011.06.002

turns out to be missing. In spectroscopic applications, the delayed acquisition is also known to result in artificially shifted spectra with distorted base lines [19].

Besides the problem of recovering the initial part of truncated FID-signals, there are situations where several parts of an NMR-signal are badly damaged by intense sporadic noise. Those parts have to be localised and restored in one way or another before any further data processing [20].

Depending on a particular application, various methods of data-processing were adopted to extract as reliably as possible physical information from truncated or impaired signals. In general, the information lost because some samples in the data-set are missing is recovered from the prior knowledge of the form of the signal to process or by making an assumption about it. Thus, various forms of the linear prediction [21–25] and, closely related to them, the 'filter diagonalisation' [26,27] – which gained favour with spectroscopists – model the regularly sampled temporal signal by a sum of complex damped exponentials – thus assuming that the spectrum of the signal contain Lorentzian lines only – and use those mathematical auto-regression properties that result from this assumption. These methods were most often used to extrapolate, explicitly or not, the final part of an FID-signal, truncated at the acquisition stage, and so to obtain spectra free of some of the faults usually caused by truncation. Some of these methods, can be used for 'line editing', to obtain a limited number of parameters of the spectral lines, i.e. their frequencies, intensities and damping factors, without calculating the spectrum properly. To our knowledge, the linear prediction was rarely applied to recover the initial part of FID-signals and, when it was, was found to be highly sensitive to noise, inextricably present in any experimental data [28,29].

Other methods were designed to calculate spectra from deliberately irregularly sampled signals. Some of them assume that the FID-signal can be modelled by a trigonometric polynomial and use the Lagrange interpolation to calculate regular samples from irregular ones, before applying a fast Fourier-transformation to them [11]. In the maximum entropy methods [30,31], on the other hand, the calculation of a spectrum is dealt with as an inverse problem in which the most regular spectrum in the entropy functional sense is chosen from those in accord with the experimental data. The multi-way decomposition methods take advantage of the fact that the spectra of three and more dimensions can be viewed as a set of direct products of their one-dimensional projections and fit the experimental data with such a product in the least square sense [32,33]. A combination of the linear prediction concepts and multi-way decomposition resulted in a spectacular decrease in the amount of experimental data necessary to calculate their spectrum [12]. More recently, spectra could be approximated from periodogrammes of the experimental data accurately enough to allow to elucidate the chemical structure of the compound under study [34,14]. Most of these methods make no assumption about the shape of the spectral lines and so have potentially a wider range of applicability than that of the methods based on the linear prediction. Nevertheless, thus obtained approximations of the spectra allow for certain faults and quantitative inaccuracies as long as it does not hinder their interpretation. Nor were they Fourier-transformed to see whether this method can be used for interpolating, extrapolating or filtering the raw data in the time domain.

A rather different class of methods that could also be used for processing truncated signals is based on their comparison with signals from data-bases. A number of packages designed for fitting the signal direct in the time domain with various model functions, yet aimed at obtaining their spectra were recently reviewed [35].

While the signals encountered in spectroscopic applications have been the subject of numerous investigations, other types of signals, e.g. those of fluids confined in porous media, have not received due attention so far. Such signals usually have no particular structure. The intrinsic difference in magnetic susceptibility of the various phases, i.e. solid matrix, confined fluid or confined gas, of the porous medium at the microscopic scale results in hugely inhomogeneous constant magnetic fields within the medium. This inhomogeneity leads to deformations and broadening of the spectral lines to up to several ppm's, with characteristic defocalisation times T_2^*'s being much shorter than the genuine spin-spin relaxation times T_2's [36,37]. Other physical systems, such as entangled polymers, are known for their non-exponential relaxation [38] and so cannot be processed by the linear prediction methods. Finally, a number of mobile NMR spectrometers were designed for in situ NMR investigations such as oil prospecting [39] or surface [40] and three-dimensional studies of bulky samples, e.g. rocks and building materials [41]. Static and RF magnetic fields produced by these spectrometers are much more inhomogeneous than those generated by the conventional NMR spectrometers and the need for the development of adequate experimental protocols for signals acquired on the mobile NMR devices has been urged in literature [42].

A typical challenge encountered in the NMR of porous media is to exactly and precisely measure the equilibrium magnetisation. As the signal defocus rapidly, taking the value of the first sample produced by the ADC for that corresponding to the beginning of the FID-signal results in great errors in the values of thus determined physical quantities. Two different strategies have been adopted to solve the problem. One consisted in using more sophisticated and longer experimental protocols rather than the single-pulse sequence. For example, to compensate the effects of magnetic-field inhomogeneity in porous materials and so to obtain images that give distribution of fluids in them precisely, transverse magnetisation could be refocused by generating spin-echoes [43,2]. The equilibrium magnetisation fields in the samples were then extrapolated from the intensities of the successive echoes' maxima assuming that relaxation is mono-exponential. The latter assumption was sometimes found to be inadequate, especially for systems where relaxation is mainly driven by molecular diffusion in the highly inhomogeneous field [43,44]. Alternatively the missing initial part of the FID-signal could be somehow calculated from the part that could be measured experimentally. Naive approaches, such as the linear extrapolation of the initial part of the FID-signal from the very first digitised samples, showed quickly their limitations, though. More sophisticated methods, usually requiring knowledge of the form of the signal and so that of the system, proved more successful. Thus the FID-signal could sometimes be supposed to have a simple mono-exponential form [45]. Nonetheless, each of these methods is suitable for processing the signals of a particular class of systems and so open no general way for the extrapolation of the initial part of an arbitrary FID-signal.

We recently proposed an algorithm for both filtering the truncated NMR data-sets in the time domain from high frequency noise and repairing an limited number of isolated samples in those sets badly damaged by intense sporadic noise [20,46]. The signal was approximated by a finite cardinal series. We supposed that the NMR-signal can often be viewed as a band-limited function, but made no other assumptions about its form. This makes it particularly suitable for processing signals of porous materials. The method proved applicable to both echoes and FID's as long as they were over-sampled.

In the present paper, we shall tackle the problem of the restoration of broad zones of impaired band-limited oversampled NMR-signals by interpolating or, in the case of the initial part of FID-signals, extrapolating them. Within the development the non-uniform sampling theory, the reconstruction of one-dimensional band-limited signals from incomplete irregular sets

of their samples was studied extensively by mathematicians [47,48]. One of the most efficient reconstruction method consists in periodically recopying the signal to reconstruct and approximating it by a series of trigonometric polynomials [49]. Unlike the approach mentioned higher [11], where the exact correspondence between the reconstructed and available samples is sought for, here one looks for a least-square approximation of the latter imposing on the frequencies of the polynomials to be regularly spread over the, supposedly continuous, spectral band of the signal to process. The method proved successful when the interval over which the signal was sampled was extensive enough and the interval between any two adjacent irregular samples was shorter than the Nyquist period of the signal, as determined by the sampling theorem [50–52]. The restoration of continuous signals from severely truncated data-sets with gaps wider than the Nyquist period, contrariwise, has received little attention, possibly because the problem of reconstruction of the continuous signal becomes intrinsically ill-conditioned, when the density of its irregular samples approaches the Nyquist frequency and any mathematical proof of numerical stability of the reconstruction is lost. Those few authors who claimed to have interpolated signals over intervals broader than the Nyquist period gave no details of their observations [53,49]. Thus, as far as we know, no quantifiable results has been reported on the performance of interpolation over broad intervals by trigonometric polynomials. Furthermore, one of the most recent reports [54] suggested that the question of the influence of the extent of truncation on the quality of reconstruction of the signal or that of mere possibility of such reconstruction are still largely neglected.

In our opinion, the reconstruction by series of trigonometric polynomials and that by cardinal series are philosophically similar, as each of the methods is based on one of the general expressions of band-limited functions. The essential difference consists in the fact that the former method requires a periodisation of the signal while the latter is free of such requirement. In the past, we already investigated the effects of the degree of truncation and that of the extension of the interval over which the signal is sampled on the performance of the cardinal series method [46] and suggested how to control these effects. To our knowledge, no similar study on the trigonometric series, which would be no doubt very useful for those concerned with processing NMR-signals, has been reported. And this is why we shall limit ourselves in this paper to the discussion of the cardinal series only.

We shall evaluate how suitable the cardinal series are for the interpolation of a large number of adjacent samples missing in the NMR-signal and that of extrapolation of the initial part of the FID-signal. Both methods can be applied to any band-limited signal, provided, as it will later transpire, their measurable parts are oversampled. Moreover the noise level of thus restored signals can turn out to be reduced compared to the original ones owing to the filtering properties of the series discussed in the past [46].

This manuscript is structured as follows: we shall first introduce some mathematical properties of the band-limited signals, which will make it easier to understand the algorithms of methods of interpolation and extrapolation of NMR-signals, whose detailed theoretical description will follow. The methods' performance and limits will then be evaluated by applying them to computer-simulated signals and compared to those of other reconstruction methods currently used by NMR-spectroscopists. Tests will focus on the size of the missing domain that can be reconstructed in relation to the size and oversampling level of available parts of the data. Finally we shall apply the extrapolation method to truncated FID-signals, experimentally acquired under conditions of highly inhomogeneous magnetic fields, to determine the equilibrium magnetisation of the sample.

2. Theory

2.1. Band-limited functions

Most analogue NMR-signals $x(t)$, should they be free of electronic noise, are band-limited functions: they have in general complex spectra $\tilde{x}(\omega)$ of a limited spectral width Ω_0 and can be expressed as

$$x(t) = \int_{\omega=-\frac{\Omega_0}{2}}^{\frac{\Omega_0}{2}} \tilde{x}(\omega)\exp(i\omega t)d\omega \tag{1}$$

Here the spectral width is defined so that $\Omega_0/2\pi$ corresponds to the 'sweep width' in Hertz in the common usage of the NMR-spectroscopists. Such functions have some remarkable properties [52]. In particular they can be expressed exactly by an infinite cardinal series (see also Fig. 1):

$$x(t) = \sum_{p=-\infty}^{\infty} a_p sinc\frac{\Omega}{2}(t-\tau_p) \tag{2}$$

where *sinc* stands for the cardinal sine function:

$$sinc(\alpha) = \frac{\sin\alpha}{\alpha} \tag{3}$$

Ω is the spectral width of the series, the quantities τ_p are moments of the time regularly spaced by a period $\delta\tau = \tau_{p+1} - \tau_p$ and the a_p are complex coefficients, which depend on Ω and τ_p, yet are almost never determined by them uniquely.

For a set of a_p to exist and so for Eq. (2) to be verified, the spectral width of the series has to be equal to or larger than that of the signal

$$\Omega \geqslant \Omega_0 \tag{4}$$

and the so called sampling frequency $\Omega_\tau = 2\pi/\delta\tau$ – the frequency at which the signal is sampled – has to be larger than a certain threshold dependent on Ω_0 and Ω, i.e.:

$$\Omega_\tau \geqslant \frac{\Omega + \Omega_0}{2} \tag{5}$$

The latter two inequalities constitute what we shall call the 'generalised Nyquist condition'. It reduces to the ordinary Nyquist condition $\Omega_\tau \geqslant \Omega_0$ when $\Omega = \Omega_0$.

The values of the signal $x(t)$ at different moments of the time t turn out to be interdependent. Indeed Eq. (2), for instance, is met when

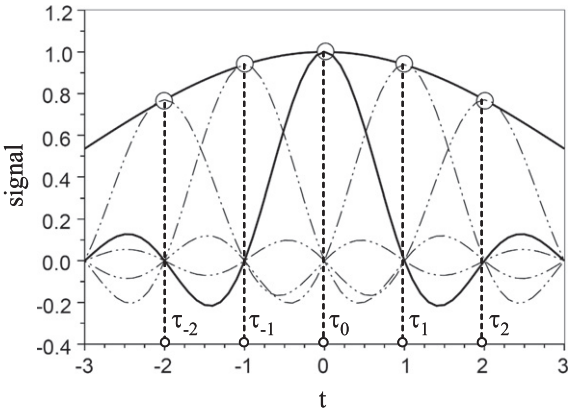

Fig. 1. Decomposition of a continuous band-limited signal (solid line) into a sum of *sinc*-functions (dotted lines); empty circles represent samples of the signal at regular moments of the time τ_p. Here $\Omega = \Omega_\tau > \Omega_0$.

$$a_p = \frac{\Omega}{\Omega_\tau} x(\tau_p) \tag{6}$$

Therefore the value of $x(t)$ at an arbitrary t can be calculated from its values at τ_p. When the signal is sampled at the Nyquist frequency, i.e. at the lowest possible frequency $\Omega_\tau = \Omega_0$ to correctly record all its harmonics, all the $x(\tau_p)$ are needed for interpolation of the signal $x(t)$ at t within intervals $\tau_p < t < \tau_{p+1}$. This is why we shall often refer hereafter to Ω_0 and $2\pi/\Omega_0$ as to Nyquist frequency and Nyquist period, respectively. If, on the other hand, the signal was oversampled, i.e. if $\Omega_\tau > \Omega_0$, the whole information about the value of the signal $x(t)$ will be encoded more than once in the values of $x(\tau_p)$. Several mathematical theorems suggest that this redundancy in $x(\tau_p)$ can be used to restore the continuous signal $x(t)$, even when a relatively large number of sequential values of $x(\tau_p)$ is missing. It is on this property of the locally oversampled band-limited functions that the methods of interpolation and extrapolation of NMR-signals proposed hereafter rely.

2.2. Signal interpolation

Let there be an arbitrary complex analogue NMR-signal $y(t)$ digitised at a finite number N of arbitrary moments of the time $t_1 < t_2 < \cdots < t_N$ to give samples $y_n = x_n + \delta x_n$, where complex $x_n = x(t_n)$ and δx_n stand for values of the noise-free signal and Gaussian non-correlated noise of the standard deviation $\sigma = \sqrt{\langle|\delta x^2|\rangle/2}$, respectively. We suggest to restore the entire analogue signal within the interval $[t_1, t_N]$ by modelling it as a finite series of truncated cardinal sine functions:

$$x(t) \approx \sum_{p=P_{inf}}^{P_{sup}} a_p sinc\frac{\Omega}{2}(t-\tau_p) \tag{7}$$

In the past we showed [20,46] that, the series of Eq. (7) approximates the modelled signal $x(t)$ within $[t_1, t_N]$ to the extent of the computer precision, when τ_p – the positions of the cardinal sine functions' maxima – are set regularly within $[\tau_{Pinf}, \tau_{Psup}] = [t_1 - 6\delta\tau, t_N + 6\delta\tau]$. Here we chose $P_{inf} = \mathrm{int}(t_1/\delta\tau) - 6$, $P_{sup} = \mathrm{int}(t_N/\delta\tau) + 6$ and $\tau_p = p\delta\tau$. In a similar way, we now suggest to set Ω and τ_p so that the generalised Nyquist condition is met and to fit the available N samples y_n with the series of the right-hand side of Eq. (7) in the least-square sense, to determine a set of values a_p:

$$Min_{a_p,(P_{inf}\leqslant p\leqslant P_{sup})} \sum_{n=1}^{N} \left| y_n - \sum_{p=P_{inf}}^{P_{sup}} a_p sinc\frac{\Omega}{2}(t_n-\tau_p) \right|^2 \tag{8}$$

and to introduce the thus found coefficients into Eq. (7) to interpolate the signal. Within the Bayesian theory for solving inverse problems [55,56], this amounts to finding maximum likelihood values of a_p.

When used for filtering band-limited NMR-signals recorded during a finite period of the time from high-frequency noise, the closer Ω is set to Ω_0 the better the filter performs, so long as the Nyquist condition is met [20,46]. More intuitively, the smaller the value of Ω, the more slowly the cardinal sine functions in the series of Eq. (7) tend towards zero when $|t_n - \tau_p|$ increases and so the more suitable they are for correlating distant samples of the signal. The period $\delta\tau$, on the other hand, was found to have no influence on the filter performance. To continue to benefit from the filtering properties of the cardinal series and to minimise the calculation time, we suggest to set the constant parameters of the cardinals series of Eq. (7) as previously:

$$\Omega_\tau = \Omega = 1.1 \times \Omega_0 \tag{9}$$

The minimum of Eq. (8) can in theory be found analytically by the pseudo-inverse method

$$A_x = \left(M_x^t M_x\right)^{-1} M_x^t Y \tag{10}$$

where A_x is a column vector whose elements constitute a set of the coefficients a_p that minimise the expression of Eq. (8)

$$A_x = \begin{pmatrix} a_{Pinf} \\ \vdots \\ a_{Psup} \end{pmatrix} \tag{11}$$

M_x is a matrix

$$M_x = \begin{pmatrix} sinc\frac{\Omega(t_1-\tau_{Pinf})}{2} & \cdots & sinc\frac{\Omega(t_1-\tau_{Psup})}{2} \\ \vdots & & \vdots \\ sinc\frac{\Omega(t_N-\tau_{Pinf})}{2} & \cdots & sinc\frac{\Omega(t_N-\tau_{Psup})}{2} \end{pmatrix} \tag{12}$$

Y is a column vector whose elements are the samples of the experimentally acquired signal

$$Y = \begin{pmatrix} y_1 \\ \vdots \\ y_N \end{pmatrix}, \tag{13}$$

The subscript x is to indicate that we deal here with reconstruction of the function $x(t)$ itself, in contrast to what will be done in the extrapolation method described in the next section. In practice, though, the matrix $M_x^t M_x$ will often be ill-conditioned, as very different sets of the coefficients a_p may lead to almost equally good approximations of the minimum [20,46]. Here we solved this problem by replacing the matrix $M_x^t M_x$ by a truncated singular value approximation [57], in which the eigenvalues smaller than the rounding error of our computer are set to zeros, while preserving all the other eigenvalues as they are. This allows to select among the various sets a_p the one of the lowest energy. Keeping in mind this substitution, we shall continue hereafter to write $M_x^t M_x$ for briefness.

After an A_x has been found, the value of the interpolated signal $s_x(t)$ as well as the standard deviation $\sigma'_x = \sqrt{\langle|\delta s_x^2|\rangle/2}$ of its Gaussian noise δs_x inherited from the Gaussian noise δx of the samples can be calculated respectively as

$$s_x(t) = V_x^t(t) A_x = V_x^t(t)\left(M_x^t M_x\right)^{-1} M_x^t Y \tag{14}$$

and

$$\frac{\sigma'_x(t)}{\sigma} = \left\| M_x \left(M_x^t M_x\right)^{-1} V_x(t) \right\| \tag{15}$$

where

$$V_x(t) = \begin{pmatrix} sinc\frac{\Omega(t-\tau_{Pinf})}{2} \\ \vdots \\ sinc\frac{\Omega(t-\tau_{Psup})}{2} \end{pmatrix} \tag{16}$$

and $\|\cdot\|$ stands for vector norm.

Thus $s_x(t)$ results from a linear transformation of y_n's and the standard deviation $\sigma'_x(t)$ of its noise depends on the moment t at which it is interpolated, the spectral width Ω of the series, the moments t_n's at which the signal was sampled by the ADC and, in theory, the locations τ_p's of the *sinc*-functions' maxima. Nevertheless, in practice, the latter were found [20,46] to have no effect as long as they were placed at a regular interval $\delta\tau$ within the interval $[t_1 - 6\delta\tau, t_N + 6\delta\tau]$.

2.3. Recovery of the absolute value of the FID-signal at the origin

Let now $y(t)$ be an FID-signal and the moment of the time t_1 at which its first sample could be produced by the ADC of the

spectrometer be strictly positive. Here t_1 corresponds to at least the 'dead time' of the spectrometer and often even a longer period [17] during which some transient phenomena hinder the start of data acquisition. One may then want to extrapolate the signal into the interval $[0, t_1]$, where zero is associated with the true beginning of the signal.

If we suppose that magnetisation was refocused at $t = 0$, then Eq. (1) assumes a particular form:

$$x(t) = \exp(i\phi)\int_{\omega=-\frac{\Omega_0}{2}}^{\frac{\Omega_0}{2}} \tilde{x}(\omega)\exp(i\omega t)d\omega \tag{17}$$

where ϕ stands for the phase that determines the direction of the RF-field in the rotating frame and the spectrum $\tilde{x}(\omega)$ is now real. The latter will usually be positive all over $[-\Omega_0/2, \Omega_0/2]$, thus corresponding to the pure absorption spectrum. Nevertheless the method described below applies even when $\tilde{x}(\omega)$ takes negative values.

Eq. (17) implies that

$$x(-t) = \exp(2i\phi)x(t)^* \tag{18}$$

where the asterisk stands for complex conjugate. This expression is purely mathematical and does not suppose that the signal $x(t)$ can be measured or even physically exists at negative t.

Let us take a simple, yet important example of an oscillating and exponentially relaxing signal $x(t > 0) = \exp(i\phi)\exp(i\omega_0 t - Rt)$, which has a pure absorption Lorentzian spectrum $\tilde{x}(\omega) = (R/2\pi)/((\omega - \omega_0)^2 + R^2)$, according to Eq. (17). This equation gives $x(t < 0) = \exp(i\phi)\exp(i\omega_0 t + Rt)$ by setting $\Omega_0 = +\infty$. The same expression can be found by using Eq. (18). The relaxation process appears to be reversed at the negative moments of the time: the signals is building up over time when $t \in [-\infty, 0]$, while it is damped down when $t \in [0, +\infty]$. On the contrary, the precession frequency ω_0 and phase ϕ are the same at negative and positive moments of the time.

The symmetry that Eq. (18) expresses allows to artificially double the number of samples in the data-set. This is now routinely employed in magnetic resonance imaging to speed up data acquisition [15]. In spectroscopy, it was combined with the linear prediction to estimate spectra in the case where signals could be measured at $t = 0$ and so where their phase ϕ was known [58].

When ϕ is indeed known, samples y_{-n} calculated at the negative moments of the time $t_{-n} = -t_n$ according to

$$y_{-n} = \exp(2i\phi)y_n^* \tag{19}$$

can be added to the set of y_n $(1 \leqslant n \leqslant N)$ and the problem of extrapolation of the signal $y(t)$ determined within $[t_1, t_N]$ into $[0, t_1]$ is effectively converted into that of interpolation of the signal determined on $[-t_N, -t_1]$ and $[t_1, t_N]$ into $[-t_1, t_1]$, discussed in the previous section.

Unfortunately, ϕ usually depends on numerous experimental factors and so is rather difficult to establish analytically. In particular, in the situation considered here, i.e. when the initial part of the FID-signal cannot be measured, the phase ϕ will be unknown. If so, the interpolation method described above cannot be applied direct to $x(t)$. Nevertheless, as $x(t)$ is a band-limited function of the spectral width Ω_0, the function $f(t) = |x(t)|^2$ is also band-limited, with the spectral width $2\Omega_0$. Moreover Eq. (18) implies that for any time:

$$|x(-t)|^2 = |x(t)|^2 \tag{20}$$

and so we can construct, noise-impaired, samples g_{-n} and g_n of $f(t)$ for negative t_{-n} and positive t_n $(1 \leqslant n \leqslant N)$ moments of the time, respectively, according to

$$g_{-n} = g_n = |y_n|^2 \tag{21}$$

and interpolate thus constructed samples of the function $f(t)$ in the interval $[-t_1, t_1]$, by setting τ_p regularly over the interval $[-t_N - 6\delta\tau, t_N + 6\delta\tau]$ and $\Omega = \Omega_\tau = 1.1 \times 2\Omega_0$. It is then possible to calculate the intensity of the FID-signal $x(t)$ in the interval $[0, t_1]$, as $|x(t)| = \sqrt{f(t)}$, without having to determine ϕ.

There is, though, an additional difficulty: the noise δf_n of the constructed samples $g_n = f_n + \delta f_n$ – inherited from the noise δx_n of the experimentally measured samples y_n's through the expression $f_n = |x_n|^2$ – is neither zero-average nor Gaussian. The mean value and the standard deviation of g_n are, respectively:

$$E(g_n) = \langle g_n \rangle = |x_n|^2 + 2\sigma^2 \tag{22}$$

$$Var(g_n) = \langle (g_n - \langle g_n \rangle)^2 \rangle = 4\sigma^2(|x_n|^2 + \sigma^2) \tag{23}$$

Moreover the noise δf_n is correlated: as $g_{-n} = g_n$, $\delta f_{-n} = \delta f_n$. Therefore, according the Bayesian theory, the fit of Eq. (7) corresponds no longer to the minimising of Eq. (8).

The probability function $p(g_n)$ of the signal $g_n = |x_n + \delta x_n|^2$ (dotted line in Fig. 2a and b) with the ratio $|x_n|/\sigma$ differs strongly from the Gaussian probability function $p_{gauss}(g_n)$ (solid line in Fig. 2a and b), i.e.

$$p_{gauss}(g_n) = \frac{1}{\sqrt{8\pi\sigma^2(|x_n|^2 + \sigma^2)}}\exp\left(-\frac{(g_n - |x_n|^2 - 2\sigma^2)^2}{8\sigma^2(|x_n|^2 + \sigma^2)}\right) \tag{24}$$

of the same mean value and standard deviation σ when $|x_n|/\sigma \ll 5$. Yet the latter can be viewed (see Fig. 2c and d) as a reasonable approximation of the former when $|x_n|/\sigma \geqslant 5$. Thus the noise δf_n can be viewed as Gaussian with the mean value $2\sigma^2$ and the standard deviation $4\sigma^2(|x_n|^2 + \sigma^2)$ when the signal $x(t)$ is measured with a relatively good signal-to-noise ratio (bigger than ten).

Given the constructed samples g_{-n} and g_n are located symmetrically with respect to zero, it is convenient to place τ_p's also symmetrically with respect to zero:

$\tau_p = \ldots, -\frac{3}{2}\delta\tau, -\frac{1}{2}\delta\tau, \frac{1}{2}\delta\tau, \frac{3}{2}\delta\tau, \ldots$ so that a_p will also be symmetrical in the fitting procedure. It then turns out possible to deal with the positive τ_p, within $[0, t_N + 6\delta\tau]$ only and to number them as follows

$$\tau_p = \left(p - \frac{1}{2}\right)\delta\tau \quad p = 1, \ldots, P_{sup} \tag{25}$$

where $P_{sup} = \mathrm{int}(1.1\Omega_0 t_N/\pi) + 6$ and $\tau_p = \pi(p - \frac{1}{2})/\Omega_0$. The approximation of Eq. (7) can then be written as

$$f(t) \approx \sum_{p=1}^{P_{sup}} a_p\left(sinc\frac{\Omega}{2}(t - \tau_p) + sinc\frac{\Omega}{2}(t + \tau_p)\right) \tag{26}$$

The advantage of this new formulation is that the values of g_n, for only positive t_n (i.e. $1 \leqslant n \leqslant N$) and impaired by uncorrelated noise are now to fit with the sum of the right-hand side of Eq. (26).

So long as the Gaussian approximation of δf_n is valid, the maximum likelihood coefficients a_P $(1 \leqslant p \leqslant P_{sup})$ are given by the generalised least-square minimisation:

$$Min_{a_p,(1\leqslant p\leqslant P_{sup})}\sum_{n=1}^{N} \times \frac{\left|g_n - 2\sigma^2 - \sum_{p=1}^{P_{sup}} a_p\left(sinc\frac{\Omega}{2}(t_n - \tau_p) + sinc\frac{\Omega}{2}(t_n + \tau_p)\right)\right|^2}{4\sigma^2(|x_n|^2 + \sigma^2)} \tag{27}$$

Approximating the unknown x_n by the measured y_n, Eq. (27) becomes

$$Min_{a_p,(1\leqslant p\leqslant P_{sup})}\sum_{n=1}^{N} \times \frac{\left|\,|y_n|^2 - 2\sigma^2 - \sum_{p=1}^{P_{sup}} a_p\left(sinc\frac{\Omega}{2}(t_n - \tau_p) + sinc\frac{\Omega}{2}(t_n + \tau_p)\right)\right|^2}{4\sigma^2(|y_n|^2 + \sigma^2)} \tag{28}$$

The analytical solution of Eq. (28) is given by

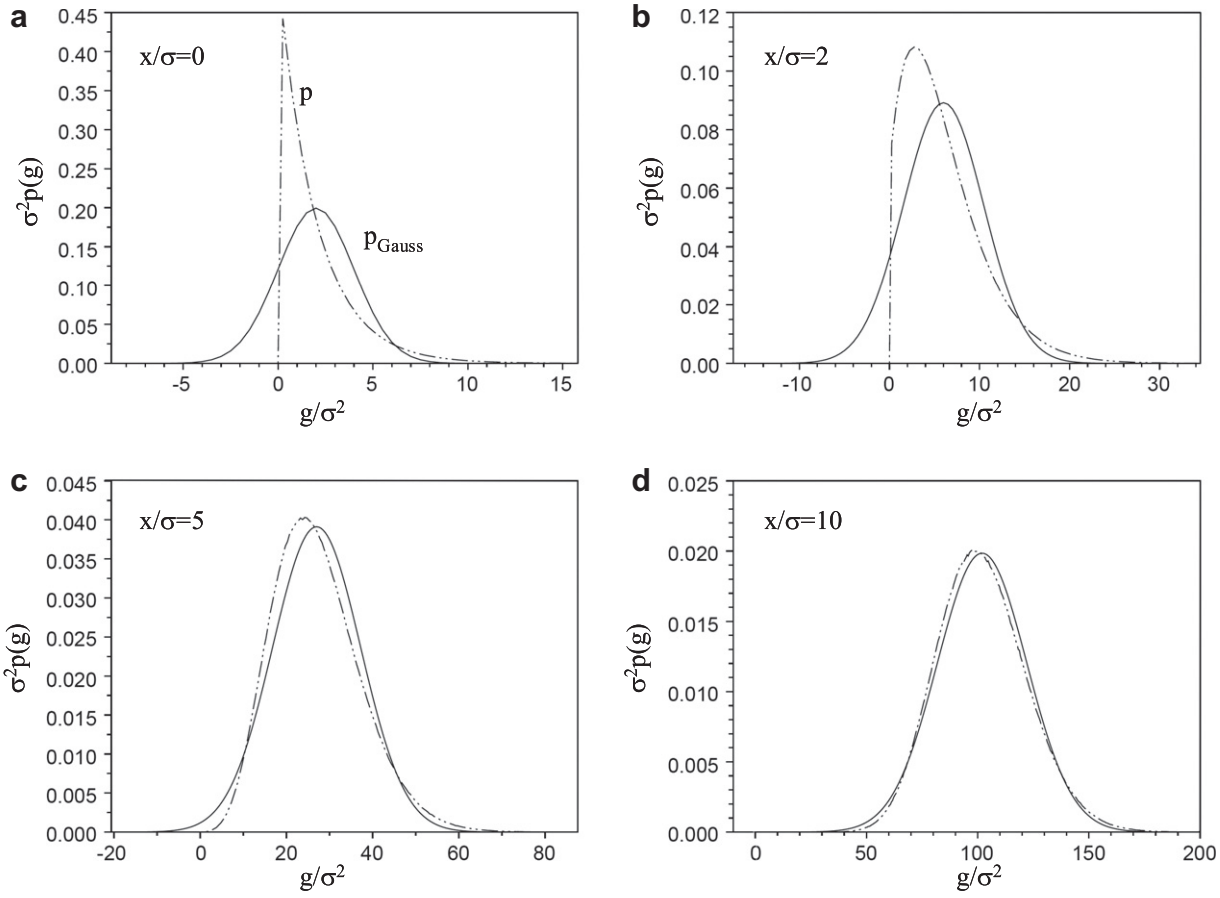

Fig. 2. Numerical estimate of the probability density $p(g)$ of the function $g = |x_n + \delta x_n|^2$ (dotted line), where x_n stands for a signal impaired by the Gaussian noise δx_n of the standard deviation σ and the ratio $|x_n|/\sigma$ equals to (a) 0, (b) 2, (c) 5 and (d) 10, and Gaussian probability function $p_{gauss}(g)$ (solid line, Eq. (24)) of the same mean value and standard deviation.

$$A_f = \left(M_f^t K^{-1} M_f\right)^{-1} M_f^t K^{-1}(G - 2\sigma^2 L), \tag{29}$$

where

$$M_f = \begin{pmatrix} sinc\frac{\Omega(t_1-\tau_1)}{2} + sinc\frac{\Omega(t_1+\tau_1)}{2}, & \cdots, & sinc\frac{\Omega(t_1-\tau_{Psup})}{2} + sinc\frac{\Omega(t_1+\tau_{Psup})}{2} \\ \vdots & & \vdots \\ sinc\frac{\Omega(t_N-\tau_1)}{2} + sinc\frac{\Omega(t_N+\tau_1)}{2}, & \cdots, & sinc\frac{\Omega(t_N-\tau_{Psup})}{2} + sinc\frac{\Omega(t_N+\tau_{Psup})}{2} \end{pmatrix} \tag{30}$$

$$K = \begin{pmatrix} |y_1|^2 + \sigma^2 & 0 & 0 \\ 0 & \ddots & 0 \\ 0 & 0 & |y_N|^2 + \sigma^2 \end{pmatrix}, \quad G = \begin{pmatrix} |y_1|^2 \\ \vdots \\ |y_N|^2 \end{pmatrix},$$
$$L = \begin{pmatrix} 1 \\ \vdots \\ 1 \end{pmatrix}, \quad A_f = \begin{pmatrix} a_1 \\ \vdots \\ a_{Psup} \end{pmatrix} \tag{31}$$

and the inverse matrix $(M_f^t K^{-1} M_f)^{-1}$ is, in practice, replaced by a truncated singular value approximation to assure against possible ill-conditioning. The subscript f is to indicate that we now deal with reconstruction of the function $f(t) = |x^2(t)|$, rather than $x(t)$ itself, as opposed to what was done in the interpolation method described in the previous section.

To interpolate $f(t)$ at a given t of $[-t_N, t_N]$, a column vector $V_f(t)$ is constructed according to

$$V(t) = \begin{pmatrix} sinc\frac{\Omega(t-\tau_1)}{2} + sinc\frac{\Omega(t+\tau_1)}{2} \\ \vdots \\ sinc\frac{\Omega(t-\tau_{Psup})}{2} + sinc\frac{\Omega(t+\tau_{Psup})}{2} \end{pmatrix} \tag{32}$$

and the value of the interpolated signal $s_f(t)$ and the standard deviation $\sigma'_f = \sqrt{\langle|\delta s_f^2|\rangle}$ of its noise δs_f, inherited from the Gaussian noise δx, can then be obtained respectively as

$$s_f(t) = V_f^t(t) A_f = V_f^t(t)\left(M_f^t K^{-1} M_f\right)^{-1} M_f^t K^{-1}(G - 2\sigma^2 L) \tag{33}$$

and

$$\sigma'_f(t) = 2\sigma\sqrt{V_f^t(t)\left(M_f^t K^{-1} M_f\right)^{-1} M_f^t K^{-1} M_f \left(M_f^t K^{-1} M_f\right)^{-1} V_f(t)} \tag{34}$$

Finally the amplitude of the signal $x(t)$ and the standard deviation of its noise can be calculated as

$$s_{|x|}(t) = \sqrt{s_f(t)} \tag{35}$$

and

$$\sigma'_{|x|}(t) = \frac{\sigma'_f(t)}{2\sqrt{s_f(t)}} \tag{36}$$

Unlike the interpolation method described in the previous section, this extrapolation method is no longer linear. Furthermore the noise level σ intervenes explicitly in the calculation of the value of the interpolated signal and so has to be determined in advance. In

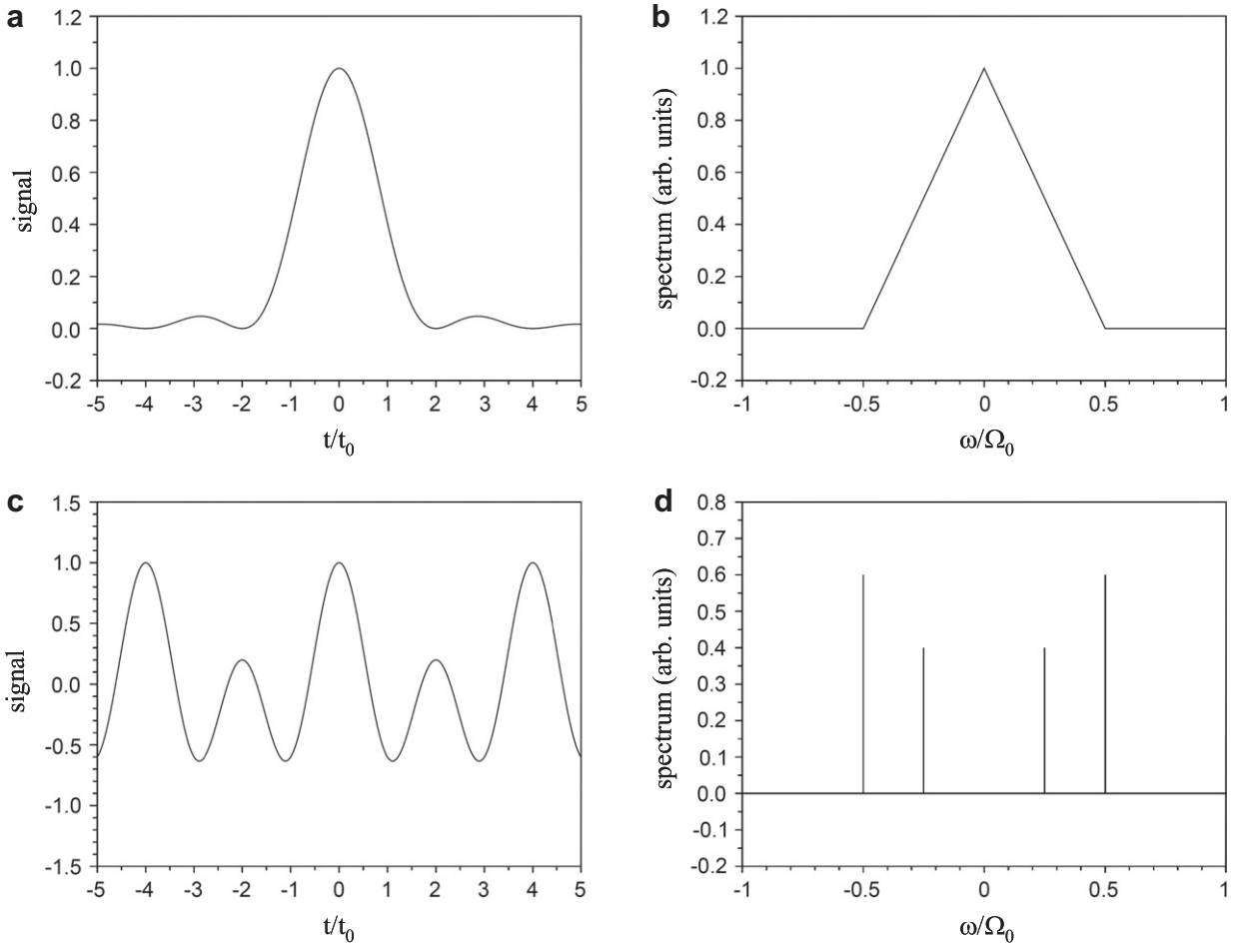

Fig. 3. Functions of Eqs. (a) (37) and (c) (38) and their Fourier-transformations, (b) and (d) respectively.

practice this can be done readily and surely by applying the method proposed previously [20] to the experimentally acquired signal itself. There σ was estimated by measuring the standard deviation of the raw (complex) data from their best fit by a band-limited cardinal series.

Finally the noise level $\sigma'_{|x|}(t)$ of the extrapolated amplitude of the experimentally acquired signal $x(t)$ depends not only on its form but also on the moments of the time t_n at which it was sampled by the ADC.

3. Results and discussion

3.1. Performance of the interpolation method

To examine its performance, the method was applied to interpolate computer-simulated noise-free signals modelled as band-limited functions

$$x(t) = sinc^2\left(\frac{\pi t}{2t_0}\right) \tag{37}$$

and

$$x(t) = \frac{3}{5}\cos\left(\pi\frac{t}{t_0}\right) + \frac{2}{5}\cos\left(\frac{\pi t}{2t_0}\right) \tag{38}$$

of the spectral width $\Omega_0 = 2\pi/t_0$ and the Nyquist period equal to t_0, the latter standing here for the time unit and will be set to one in all that follows. These two functions are somewhat reminiscent of echo signals (see Fig. 3a and c respectively), with a broad spectrum (see Fig. 3b) in the case of the former and with a spectrum consisting of four infinitely narrow spectral lines (see Fig. 3d) in the case of the latter. Both functions take the value of one at $t = 0$.

Fig. 4 shows the result of the reconstruction of the continuous signal of Eq. (38) within the interval $[-5t_0, 5t_0]$ from its forty regular samples within the intervals $[-3t_0, -t_0]$ and $[t_0, 3t_0]$, either noise-free (on the left) or impaired by Gaussian noise of the standard deviation $\sigma = 0.001$ (on the right), by the cardinal series method (on the top), Lagrange interpolation as described in literature [11] (in the middle) or modified by us (on the bottom). The linear prediction cannot be applied here as the absence of samples within the interval $[-t_0, t_0]$ breaks regularity of the sampling. The continuous signal (dotted lines in Fig. 4a and b) was precisely reconstructed (solid lines in the same figure) within the interval $[-3t_0, 3t_0]$ by the cardinal series method even in the presence of noise. Contrariwise our method fails to reconstruct the signal at t smaller than $-3t_0$ and bigger than $3t_0$ and so proves unsuitable for extrapolating signals. The Lagrange interpolation as described in literature, on the other hand, was inept to reconstruct the analogue signal even within the intervals $[-3t_0, -t_0]$ and $[t_0, 3t_0]$ of regular sampling and in the absence of noise (Fig. 4c and d). We see at least two reasons for this failure: there are no samples in the vicinity of $t = 0$, whilst it was suggested to be a prerequisite [11]; moreover, the method imposes no condition on the spectral width of the signal to reconstruct, which, we believe, is essential for the approximation to converge. The latter aspect will be discussed in detail in Appendix, where we also propose a modification of the Lagrange method that takes into account the spectral width of the signal. The modified version of the Lagrange method is fairly satisfying

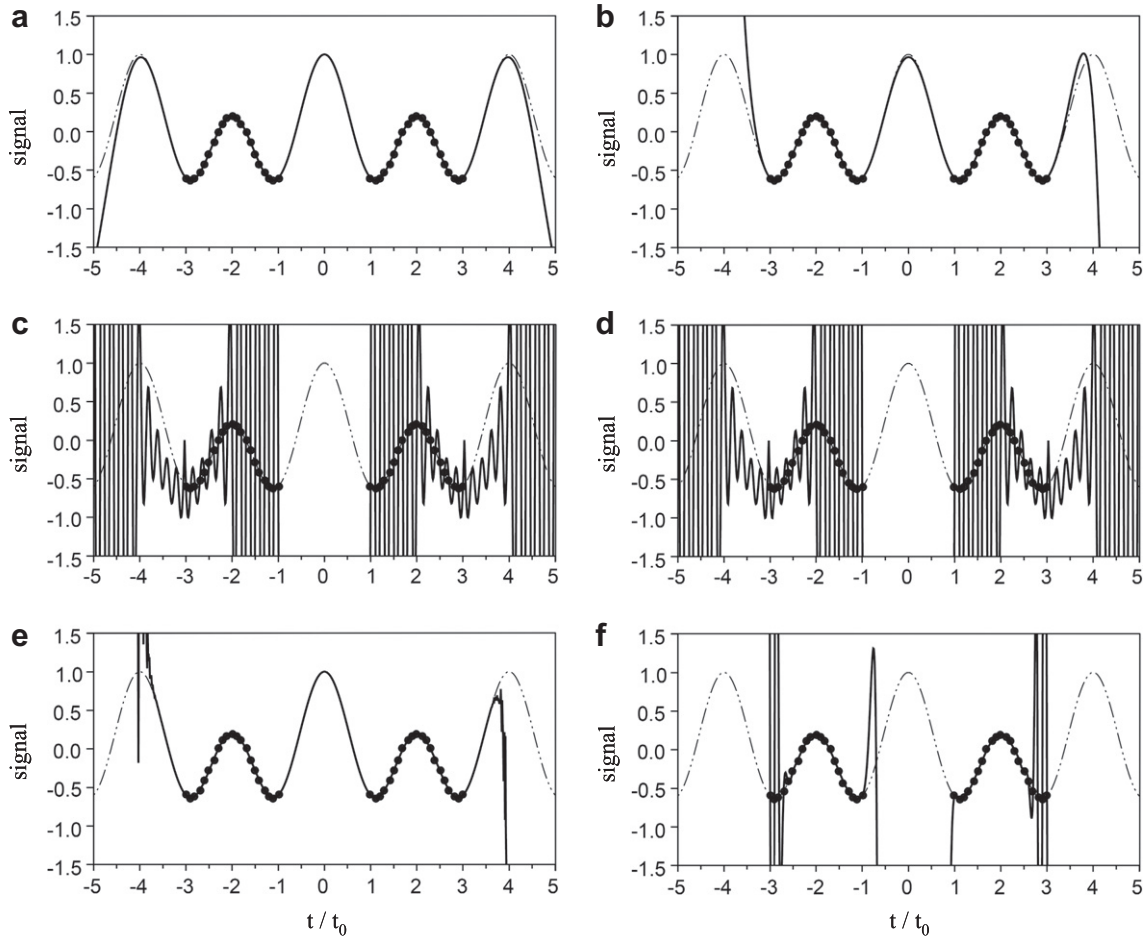

Fig. 4. Interpolation (continuous line) of the continuous signal (dot-dashed line) of Eq. (38), either noise-free (on the left) or impaired by Gaussian noise of standard deviation $\sigma = 0.001$ (on the right), from its forty regular samples (filled circles) within the intervals $[-3t_0, -t_0]$ and $[t_0, 3t_0]$ by using cardinal series (on the top) or the Lagrange interpolation method as described in literature (in the middle) and as modified by us (on the bottom).

when allied to the noise-free signal within the interval $[-3t_0, 3t_0]$ (Fig. 4e), but turns out to be unstable with respect to noise (Fig. 4f).

We put our method to further tests to be able to assess its stability. In the first test, the functions of Eqs. (37) and (38) were sampled regularly, at the frequency Ω_S set to ten times the spectral width of the functions Ω_0, within the domains of the type $[-t_{inf} - \Delta t, -t_{inf}] \cup [t_{inf}, t_{inf} + \Delta t]$, where varied $t_{inf} \geqslant 0$ and $\Delta t \geqslant 0$, and were interpolated into the intervals $[-t_{inf}, t_{inf}]$.

The difference $|s_x(t = 0) - 1|$ between the value of the noise-free signals of Eqs. (37) (see Fig. 5a) and (38) (see Fig. 5b) obtained by interpolation and their theoretical value – which reflects the intrinsic bias of the method – were calculated at $t = 0$ as a function of t_{inf} and Δt varied within $[0, 5t_0]$ and $[0.1t_0, 100t_0]$, respectively.

Left of the darker solid line in Fig. 5a and b, the bias does not exceed 1%, which, we think, is very satisfying, as this will usually correspond to the relative error with which one can reasonably hope to measure NMR-signals. Not surprisingly, for the intervals $[-t_{inf}, t_{inf}]$ narrower than the Nyquist period, i.e. for $t_{inf} < t_0/2$, this bias decreases below 10^{-5}, becoming comparable with the rounding error encountered when the cardinal series was used to filter signals sampled over continuous intervals [46].

The width $2t_{inf}$ of the interval into which the signals can be interpolated turns out to strongly depend on the extent Δt of interval over which the signal was sampled. For small Δt, the interpolation was successful for the width $2t_{inf}$ hardly broader than the Nyquist period of the signals. When Δt increases, i.e. when there are more available samples of the signal and so more information about it, it can be interpolated into intervals whose width is several times the Nyquist period, i.e. $t_{inf} \gg t_0/2$.

A closer look reveals dependence of the method's bias on the form of the signal. The signal of the form of Eq. (37) could be interpolated into an interval up to almost ten times broader than its Nyquist period, i.e. for $t_{inf}/t_0 \approx 5$, when $\Delta t = 100t_0$ (see Fig. 5a). The signal of the shape given by Eq. (38), contrariwise, could be interpolated into an interval no broader than five times its Nyquist period, i.e. for $t_{inf}/t_0 \approx 2.5$, when $\Delta t \geqslant 3t_0$ (see Fig. 5b); and this limit could not be raised by further increasing Δt. Note (Fig. 5a) that a similar feature occurred when Δt was raised to $20t_0$ or higher.

In the context of regular sampling of band-limited signals the Nyquist period is often associated with the maximal sampling period that allows to reconstruct the continuous signal from its samples. The results of the tests summed up in Fig. 5a and b shows that the continuous signal can actually be reconstructed from its irregular samples some of which located several Nyquist periods apart from one another provided that there are enough other samples placed closer to each other than the Nyquist period.

We also studied the dependence of the noise amplification σ'_x/σ, defined by Eq. (15), on t_{inf} and Δt. When the interval into which the signal has to be interpolated is narrower (see Fig. 5c) than one Nyquist period, and when Δt is slightly higher than t_0, then $\sigma'_x/\sigma \leqslant 1$, which means that the interpolated signal is impaired by noise of lower level than the experimentally acquired signal from which it was interpolated. Therefore, along with

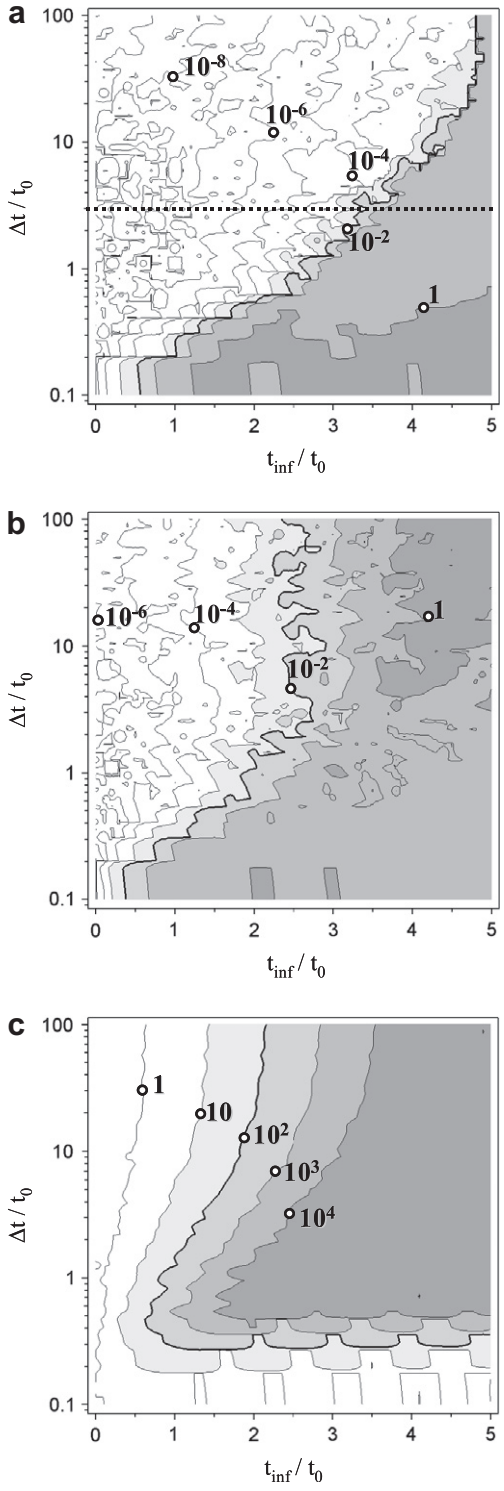

Fig. 5. Difference $|s_x(t=0)-1|$ between the value of the functions of Eqs. (a) (37) and (b) (38) obtained by interpolation and their theoretical value at $t=0$, one, as a function of t_{inf} and Δt varied within $[0, 5t_0]$ and $[0.1t_0, 100t_0]$, respectively, for $\Omega_s = 10\Omega_0$; (c) noise amplification σ'_x/σ as a function of the same parameters.

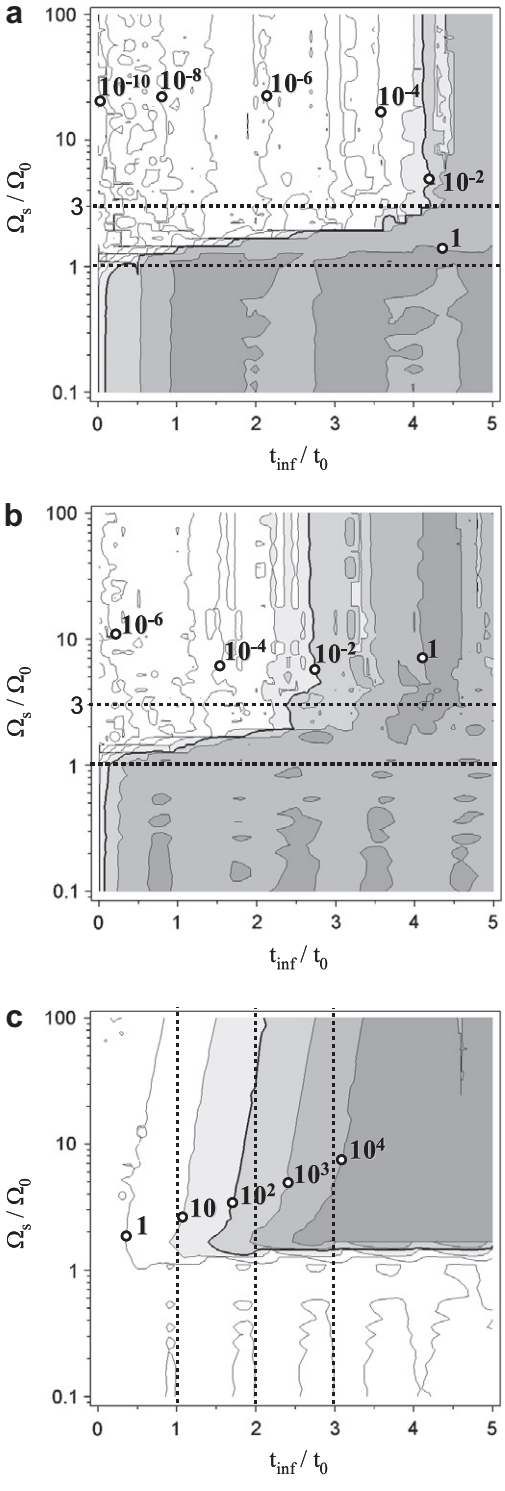

Fig. 6. Difference $|s_x(t=0)-1|$ between the value of the functions of Eqs. (a) (37) and (b) (38) obtained by interpolation and their theoretical value at $t=0$, one, as a function of t_{inf} and Ω_s varied within $[0, 5t_0]$ and $[0.1\Omega_0, 100\Omega_0]$, respectively, for $\Delta t = 10t_0$; (c) noise amplification σ'_x/σ as a function of the same parameters.

interpolation, the signal benefits from the filtering properties of the cardinal series established in the past [20,46]. When the interpolation interval increases, noise propagated through the interpolation procedure rises quickly by orders of magnitude. Thus noise amplification appears as another possible factor limiting the width of the interpolation interval. One can assume that the interpolation will be successful in the area left of the solid line in Fig. 5c, where $\sigma'_x/\sigma \leqslant 100$, given the signal-to-noise ratio of experimentally acquired signals seldom exceeds ten thousand. Here once again broader interpolation intervals can be achieved by broadening Δt; and for $\Delta t = 100t_0$ the interpolation interval can be as broad as four Nyquist periods.

Clearly, oversampling the signal in the domain $[-t_{inf} - \Delta t, -t_{inf}] \cup [t_{inf}, t_{inf} + \Delta t]$ is absolutely necessary for being able to interpolate it into an interval $[-t_{inf}, t_{inf}]$ broader than its Nyquist period.

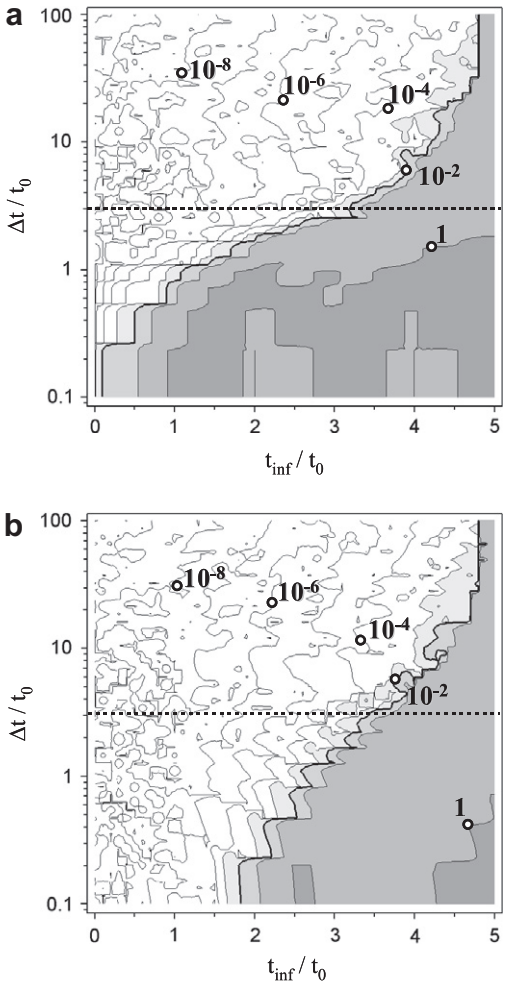

Fig. 7. Difference $|s_x(t=0)-1|$ between the value of the function of Eq. (37) obtained by extrapolation and their theoretical value at $t=0$, one, as a function of t_{inf} and Δt varied within $[0, 5t_0]$ and $[0.1t_0, 100t_0]$, respectively, for (a) $\Omega_S = 4\Omega_0$ and (b) $\Omega_S = 100\Omega_0$.

In the second test, to understand the influence of the sampling frequency Ω_S, we studied the bias of the interpolation of the signals of the form of Eqs. (37) and (38) as a function of the interpolation interval t_{inf}, varied within $[0, 5t_0]$, at different sampling frequencies within $[0.1\Omega_0, 100\Omega_0]$, while Δt was set to $10t_0$ (Fig. 6a and b respectively). Fig. 6c shows the noise amplification σ'_x/σ as a function of the same parameters. The charts for both types of signal are similar. When $\Omega_S < \Omega_0$, the signal is under sampled and any attempt to interpolate it fails. When $\Omega_S > 3\Omega_0$, the signal is oversampled enough for interpolation to succeed. Naturally, there is then still a certain limit to how wide the interval where samples of the signal were not available can be for interpolation to be successful. This limit does not depend on Ω_S but on the form of the processed signal: it is equal to eight Nyquist periods for the signal of Eq. (37) (Fig. 6a) and five Nyquist periods for the signal of Eq. (38) (Fig. 6b). Finally, when $\Omega_0 < \Omega_S < 3\Omega_0$, narrowness of t_{inf} becomes crucial to the success of interpolation.

Finally we investigated the performance of our interpolation method applied to the signal of Eq. (37) as a function of Δt and t_{inf} when the sampling frequency Ω_S is comparable with ($\Omega_S = 4\Omega_0$, Fig 7a) or much higher ($\Omega_S = 100\Omega_0$, Fig 7b) than the spectral width of the signal Ω_0. The case of an intermediate value of the sampling frequency, i.e. $\Omega_S = 10\Omega_0$, was shown in Fig. 5a. When $\Delta t < 3t_0$, i.e. when only a very limited number of samples are available, increase in Ω_S improves tremendously the quality of interpolation.

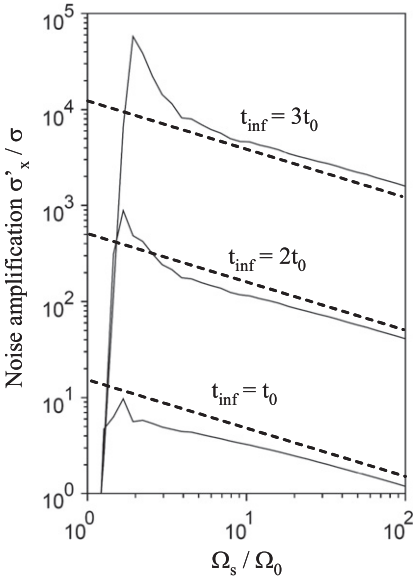

Fig. 8. Evolution of noise amplification σ'_x/σ as a function of Ω_s while t_{inf} was set to t_0, $2t_0$ and $3t_0$ and $\Delta t = 10t_0$. The graph is an arrangement of the three planar cross-sections (dotted lines in Fig. 6c) of the diagram of Fig. 6c. Dotted lines to guide the viewer have tangent of $-1/2$.

When $\Delta t > 3t_0$, on the other hand, all the three charts are almost identical. Thus, except for extremely truncated signals, raising Ω_S further than $4\Omega_0$ proves to have no effect on either the interpolation exactitude or the maximal width of the interpolation interval. Nevertheless Fig. 6c shows that, when the interpolation is possible, a rise in Ω_S results in substantial decrease of σ'_x/σ. Fig. 8 shows that σ'_x/σ then depends on the sampling frequency as $\Omega_S^{-1/2}$ independently of t_{inf}. Thus, raising Ω_S results in lowering the noise level by a factor of $\sqrt{\Omega_s}$ and can be useful when acquiring signal with a low signal-to-noise ratio.

3.2. Performance of the extrapolation method

We wanted to compare our extrapolation method with that of the linear prediction. To be able to do so, we had to choose a regular data-set. Fig. 9 shows the reconstruction of the continuous signal of Eq. (37) within the interval $[0, 3t_0]$ from its twenty regular samples within the interval $[t_0, 3t_0]$, either noise-free (on the left) or impaired by Gaussian noise of the standard deviation $\sigma = 0.001$ (on the right), by the cardinal series method (on the top) and by one of the numerous linear prediction methods [21–25], i.e. Iterative Quadratic Maximum Likelihood (IQML) (on the bottom). The IQML was chosen as it was shown to be the most stable and reliable among the linear prediction methods for calculating NMR-spectra of biological polymers [25]. Moreover, this particular linear prediction method is the only one that sets all the parameters of the prediction model by a least-square fit of the data, which is the proper way of dealing with the inverse problems from the point of view of the Bayesian theory when the data is affected by Gaussian noise [55,56].

The cardinal series method extrapolated the initial part of the FID-like signal beautifully (Fig. 9a) even in the presence of noise (Fig. 9b). The IQML also proved highly successful in extrapolation the initial part of the noise-free signal (Fig. 9c), yet failed miserably when applied to the signal impaired by a moderate noise (Fig. 9d). Thus we recover here the conclusion, drawn in the past [30], that the linear prediction cannot be viewed as a reliable mean of extrapolation of the signal in the time domain, even though it does alleviate considerably the adverse effects of truncation on the signal in the frequency domain.

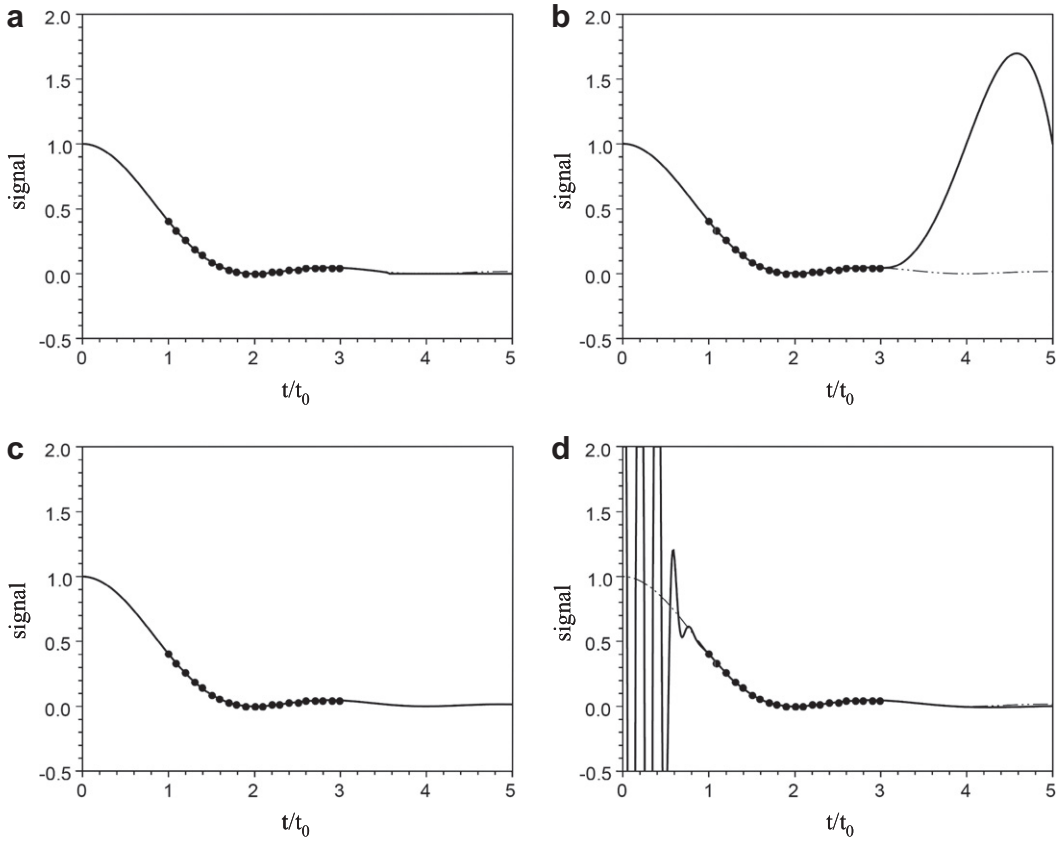

Fig. 9. Extrapolation (solid line) of the continuous signal (dot-dashed line) of Eq. (37), either noise-free (on the left) or impaired by Gaussian noise of standard deviation $\sigma = 0.001$ (on the right), from its twenty regular samples (filled circles) within the interval $[t_0, 3t_0]$ by using cardinal series (on the top) and the IQML method (on the bottom).

We put our extrapolation method, described in Section 2.3, to the tests similar to those of the previous section. In the first test, the functions of Eqs. (37) and (38) were sampled regularly within the intervals $[t_{inf}, t_{inf} + \Delta t]$ at the frequency $\Omega_S = 10\Omega_0$ and extrapolated into the intervals $[0, t_{inf}]$. Thus modelled signals have real spectra (see Fig. 3) and so satisfy the conditions of the method's applicability, and noise-free. Nevertheless it is necessary to specify a noise level σ, as it now intervenes in the calculation (see Eq (28)). In what follows, we report tests performed for $\sigma = 0.0001$, a value similar to that encountered in our experiments (see Section 3.3).

The charts of Fig. 10a and b show evolution of the bias $|s_{|x|}(t = 0) - 1|$ of extrapolation of the model signals as a function of t_{inf} and Δt gradually varied within $[0, 2.5t_0]$ and $[0.1t_0, 100t_0]$ respectively, while those of Fig. 10c and d show the noise amplification $\sigma'_{|x|}/\sigma$. The charts in Fig. 10a and b reveal patterns similar to those of Fig. 5a and b, though, scaled down by a factor of two or so in the t_{inf} direction. This comes as no surprise given the close relationship between the extrapolation and interpolation methods. The extrapolation method consists in transforming the problem of extrapolation of a signal with the spectral width Ω_0 into the problem of interpolation of its squared norm, of the spectral width $2\Omega_0$, and so a contraction by a factor of two is to be expected. The difference between the expected and actually observed scaling factors can be accounted for by difference in the inherent dependence of the interpolation and extrapolation methods on the form of the processed signal. The charts in Fig. 10c and d confirm that the noise-level amplification of the extrapolation method also depends on the shape of the signal. This amplification is smaller that one in a upper left zone in Fig. 10c and d, which means that, along with extrapolation, the signal will continue to benefit from filtering properties of the cardinal series.

Other tests, on other types of band-limited signal with σ ranging from 0.0001 to 0.1 (not shown here), confirm the general character of these observations, which can be summed up as follows: while the interpolation method requires that $\Omega_S > 3\Omega_0$, the extrapolation methods necessitates that $\Omega_S > 6\Omega_0$; the maximal t_{inf} for which extrapolation is successful is about two times smaller than that for which interpolation is possible. In general as long as the domain Δt over which the signal was sampled exceeds a few Nyquist periods t_0, the signal can be extrapolated into the interval $[0, t_{inf}]$ of the width t_{inf} at least as broad as $t_0/2$, which ranges here between $1.3t_0$ for signal (38) and $1.8t_0$ for signal (37) whatever systematic bias or noise amplification are considered (bold lines in Fig. 10). This is quite remarkable, as this means that the absolute value of the signal can be interpolated into the interval $[-t_{inf}, t_{inf}]$ seven times of its own Nyquist period $t_0/2$.

3.3. Application of the extrapolation method to experimentally acquired signals

Finally, to further underline usefulness and explore capacity and limits of our extrapolation method we applied it to experimentally acquired signals.

Twenty-one water-proton FID-signals of a 60 ml sample of the 10^{-2} mol/l aqueous solution of $CuSO_4$ were generated by the experimental scheme of Fig. 11 in which magnetic field gradient was incremented in 21 steps from one experiment to another to gradually broaden the spectrum of thus defocused signal from 300 Hz to 10 kHz. The signal-to-noise ratio was not less than 5000. We assured that all signals were sampled at least ten times

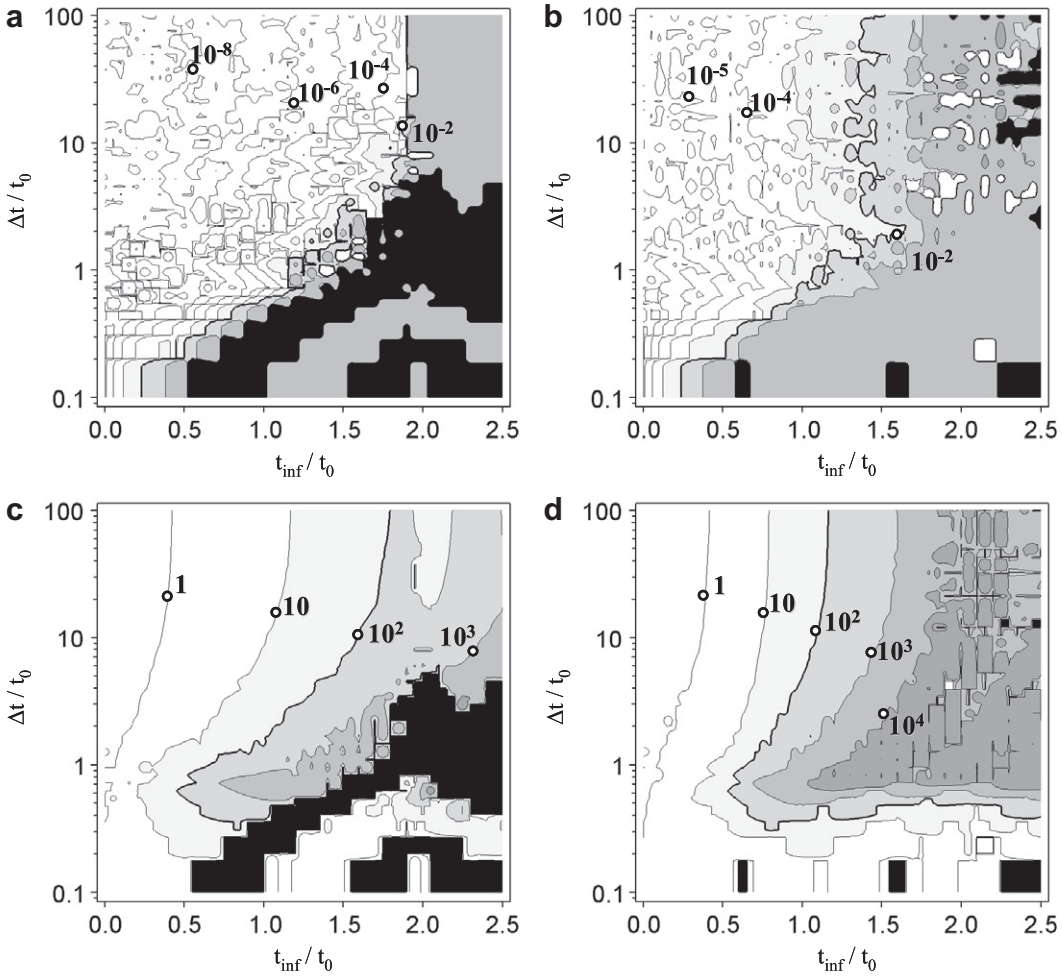

Fig. 10. Difference $|s_{|x|}(t=0)-1|$ between the value of the signals of Eqs. (a) (37) and (b) (38) obtained by extrapolation and their theoretical value at $t=0$, one, as a function of t_{inf} and Δt varied within $[0, 2.5t_0]$ and $[0.1t_0, 100t_0]$, respectively, for $\Omega_s = 10\Omega_0$; noise amplification $\sigma_{|x|}/\sigma$ of the signals of Eqs. (c) (37) and (d) (38) as a function of the same parameters. The zones of utter failure of the method (leading to negative extrapolated squared signal intensity) are coloured in black.

more frequently than required by the Nyquist criterion by setting the sampling frequency to 100 kHz. The initial 330 μs long part of each of the FID-signals was interfered by the parasite signal stemming from the sample-holder and so had first to be chopped off and then extrapolated from the rest of the signal. Fig. 12a shows the result of extrapolation of three of the 21 signals into the initial 330 μs as well as the three truncated experimentally acquired signals themselves. As one would expect it from the signals measured on the same sample, all extrapolated signals have the same amplitude at $t = 0$, associated here as usual with middle of the last RF-pulse in the experiment.

Fig. 12b shows the intensity of the first sample (at $t = 330$ μs) of the truncated FID-signals as well as the intensity of the extrapolated signals at $t = 0$ as a function of the spectral width of the signal. The former, as could be expected, decreases quickly when the spectral width increases, while the latter stays unchanged until the spectral width reaches the value of 5 kHz, thus confirming the most satisfying performance of the extrapolation method. The method fails when applied to signals with spectra broader than 5 kHz and so with the Nyquist periods smaller than 200 μs. This corresponds to the ratio of the length of the interval into which the signal is to extrapolate and the signal's Nyquist period of 1.65 and is in good accord with the results of Fig. 10, where the extrapolation method failed when t_{inf} exceeded a certain threshold within the interval $1.3t_0 \leqslant t_{inf} \leqslant 1.8t_0$ for Δt bigger than few t_0.

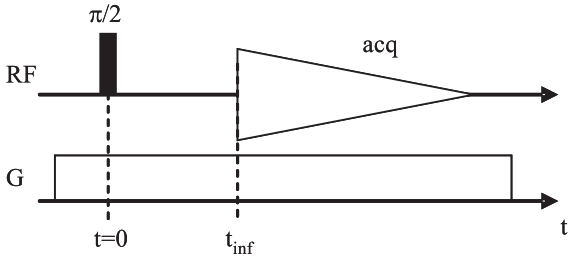

Fig. 11. Pulse sequence used to measure signals of the aqueous solution of $CuSO_4$; gradient allowed to change at will the spectral width of the signal.

Finally Fig. 13 shows the result of extrapolation of the initial 600-μs long parts of the water-proton FID-signals – acquired in single-pulse experiment – of the same quantity of distilled water in a flask either filled or not with glass beads of various diameters. The signals, of the spectral width of 1 kHz and 300 Hz, were both sampled at 100 kHz. Here again, despite the significantly faster decrease of the signal in the porous system compared with that of the pure water, the amplitudes of the two extrapolated signals show a relative discrepancy of only 1.6%. This confirms the ability of our extrapolation method to compensate for the effects of magnetic-field inhomogeneity and thus to allow precise measurement of amount of water in porous media.

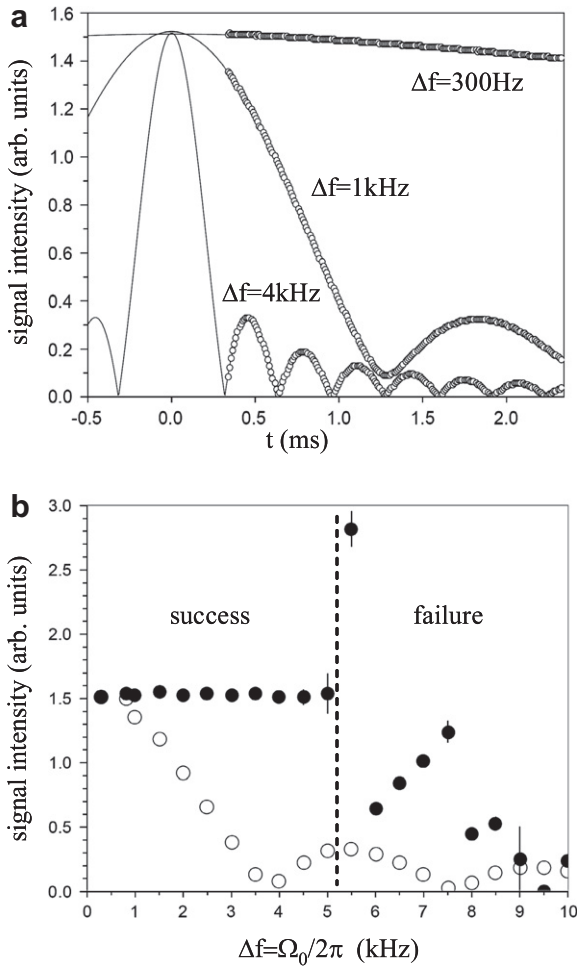

Fig. 12. (a) FID-signals of the spectral width of $\Delta f = 300$ Hz, 1 kHz and 4 kHz extrapolated into [0, 330 μs] (solid line) from their regular samples within [330 μs, 3000 ms] (white circles) measured with the pulse sequence of Fig. 10; (b) intensities of the first sample (empty circles) of the truncated FID-signals measured at $t = 330$ μs in the experiments of Fig. 10 and those determined at $t = 0$ by extrapolation (filled circles) as a function of the spectral width.

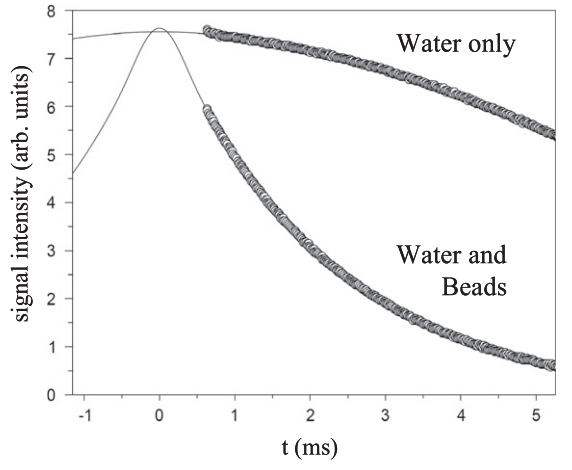

Fig. 13. Intensities of the measured (white circle) and extrapolated (solid line) FID-signals of the same quantity of distilled water in a flask either filled or not with glass beads of various diameters.

4. Conclusions

We proposed two methods of restoring missing parts of incomplete NMR-signals dominated by effects of field inhomogeneity. Unlike most NMR-data processing techniques currently used in spectroscopy, these methods do not rely on any model of NMR-signal and require nothing but the signal to be a band-limited function and its available parts oversampled.

One of the methods allows to interpolate the incomplete signal into intervals many times broader than its Nyquist period. Another permits to extrapolate the amplitude of the initial missing part of the refocussed FID-signal. The both methods necessitate that domains in which the signal is to be reconstructed are juxtaposed with those where it is oversampled. The broader are the domains of oversampling, the better is the performance of the methods. Performance of the methods were shown by applying them to experimentally acquired signals. Our methods proved much more stable than those of the linear prediction or Lagrange interpolation.

We believe that, for NMR-studies in civil engineering, our methods may be useful alternatives to those used most often in NMR-spectroscopy.

5. Experimental

All numerical simulations, calculations and data-processing algorithms were coded in both FORTRAN 95 and Scilab programming languages.

The water-proton NMR-experiments were carried out on a 60 ml sample of the 10^{-2} mol/l aqueous solution of $CuSO_4$ and on a 25 ml sample consisting of glass beads of diameter ranging between 128 and 166 μm bunched together and immersed in distilled water at a vertical Bruker 24/80 Avance DBX MRI spectrometer equipped with a 20 cm birdcage RF-coil and operating at the field 0.5 T with maximal gradient of 5 G/cm.

Acknowledgments

This work was supported by the Agence Nationale de la Recherche (ANR) of France through the ANR-06-JCJC-0106 project managed by Dr Teddy Fen Chong.

Appendix A. Lagrange Interpolation with spectral-band control

In the adaptation [11] of the Lagrange interpolation [59], the interval $[t_1, t_N]$ over which a set of samples x_n is collected at the moments of the times $t_1 < t_2 < \cdots t_N$ is rescaled into the non-dimensional interval $[-\pi, \pi]$ by the affine transformation

$$t_n \to \tilde{t}_n = \frac{2\pi}{t_N - t_1}\left(t_n - \frac{t_N + t_1}{2}\right) \tag{A1}$$

The signal to reconstruct is modelled by the trigonometric series

$$x(t) = \sum_{k=-N/2}^{N/2-1} \alpha_k \exp(ik\tilde{t}) \tag{A2}$$

By setting $z = \exp(i\tilde{t})$, Eq. (A2) can be expressed as

$$x(t) = z^{-N/2} \sum_{k=0}^{N-1} \alpha_{k-N/2} z^k = z^{-N/2} \times P(z), \tag{A3}$$

where $P(z)$ is a polynomial of the degree N−1 of the complex argument z which has to be adjusted so that $P(z_n) = x(t_n) \times z_n^{N/2}$ for $z_n = \exp(i\tilde{t}_n)$. Finally we obtain an efficient reconstruction expression

$$x(t) = z^{-N/2} \sum_{n=1}^{N} x(t_n) z_n^{N/2} \prod_{j=1, j\neq n}^{N} \frac{z - z_j}{z_n - z_j} \tag{A4}$$

It is by using this relationship that Fig. 4c and d were obtained.

The band-width of the reconstructed signal can be determined by introducing (A1) into (A2):

$$x(t) = \sum_{k=-N/2}^{N/2-1} \alpha_k \exp\left(ik\frac{2\pi}{t_N - t_1}\left(t - \frac{t_N + t_1}{2}\right)\right) \quad \text{(A5)}$$

Hence the oscillation frequencies of the complex exponentials used for reconstruction are regularly spread over the spectral band $[-\Delta\omega/2, \Delta\omega/2]$ with

$$\Delta\omega = 2\pi\frac{N}{t_N - t_1} \quad \text{(A6)}$$

In the example of Fig. 4 of the Lagrange interpolation, the spectral width of the approximation function was made much wider than the spectral width of the signal, i.e. $\Delta\omega = 6.7\Omega_0$. This, no doubt, took its toll of quality of the interpolation.

As an improvement, we suggest to take into account the true spectral band of the signal by replacing Eq. (A1) by

$$t_n \to \tilde{t}_n = \frac{\Omega_0}{N}\left(t_n - \frac{t_N + t_1}{2}\right) \quad \text{(A1bis)}$$

So long as the mean density $N/(t_N - t_1)$ of samples in $[t_1, t_N]$ is higher than the Nyquist frequency $\Omega_0/2\pi$, this relation will transform the interval $[t_1, t_N]$ into an interval inside $[-\pi, \pi]$, and we can continue to use Eq. (A4) being sure that the spectral width of the approximation function will be set exactly to that of the signal to interpolate. It is by using this relationship that Fig. 4e and f were obtained.

References

[1] P.F. Faure, S. Caré, C. Po, S. Rodts, Magn. Reson. Imaging 23 (2005) 311–314.
[2] L. Li, H. Han, B.J. Balcom, J. Magn. Reson. 198 (2009) 252–260.
[3] J.H. Strange, Int. J. Nondestr. Test 11 (1994) 261–271.
[4] R.M.E. Valckenborg, L. Pel, K. Kopinga, Magn. Reson. Imaging 19 (2001) 489–491.
[5] H.Y. Carr, E.M. Purcell, Phys. Rev. 94 (1954) 630–638.
[6] S. Meiboom, D. Gill, Rev. Sci. Instrum. 29 (1958) 688–691.
[7] E.O. Stejskal, J.E. Tanner, J. Chem. Phys. 42 (1965) 288–292.
[8] J.E. Tanner, J. Chem. Phys. 52 (1970) 2523–2526.
[9] H. Gesmar, J.J. Led, J. Magn. Reson. 83 (1989) 53–64.
[10] J.C.J. Barna, E.D. Laue, M.R. Mayger, J. Skilling, S.J.P. Worrall, J. Magn. Reson. 73 (1987) 69–77.
[11] D. Marion, J. Biomol. NMR 32 (2005) 141–150.
[12] V. Jaravine, I.V. Ibraghimov, V.Y. Orekhov, Nat. Methods 3 (2006) 605–607.
[13] J.C. Hoch, M.W. Maciejewski, B. Filipovic, J. Magn. Reson. 193 (2008) 317–320.
[14] K. Kazimierczuk, A. Zawadzka, W. Kozminski, J. Magn. Reson. 197 (2009) 219–228.
[15] D.A. Feinberg, J.D. Hale, J.C. Watts, L. Kaufman, A. Mark, Radiology 161 (1986) 527–531.
[16] N.K. Chen, K. Oshio, L.P. Panych, Magn. Reson. Med. 59 (2008) 916–924.
[17] D. Bytchenkoff, G. Bodenhausen, J. Magn. Reson. 165 (2003) 1–8.
[18] G. Bodenhausen, Personal Communication.
[19] C. Tang, J. Magn. Reson. A 109 (1994) 232–240.
[20] D. Bytchenkoff, S. Rodts, P. Moucheront, T. Fen-Chong, J. Magn. Reson. 202 (2010) 147–154.
[21] H. Barkhuijsen, R. De Beer, D. Van Ormondt, J. Magn. Reson. 73 (1987) 553–557.
[22] M.-A. Delsuc, F. Ni, G.C. Levy, J. Magn. Reson. 73 (1987) 548–552.
[23] J. Tang, J.R. Norris, J. Magn. Reson. 78 (1988) 23–30.
[24] C.F. Tirendi, J.F. Martin, J. Magn. Reson. 85 (1989) 162–169.
[25] G. Zhu, W.Y. Choy, B.C. Sanctuary, J. Magn. Reson. 135 (1998) 37–43.
[26] V.A. Mandelshtam, J. Magn. Reson. 144 (2000) 343–356.
[27] G.S. Armstrong, V.A. Mandelshtam, J. Magn. Reson. 153 (2001) 22–31.
[28] D. Marion, A. Bax, J. Magn. Reson. 83 (1989) 205–211.
[29] H. Hu, Q.N. Van, V.A. Mandelshtam, A.J. Shaka, J. Magn. Reson. 134 (1998) 76–87.
[30] A.S. Stern, K.-B. Li, J.C. Hoch, J. Am. Chem. Soc. 124 (2002) 1982–1993.
[31] M. Mobli, M.W. Maciejewski, M.R. Gryk, J.C. Hoch, J. Biomol. NMR 39 (2007) 133–139.
[32] D.M. Korzhnev, I.V. Ibraghimov, M. Billeter, V.Y. Orekhov, J. Biomol. NMR 21 (2001) 263–268.
[33] T. Luan, V. Jaravine, A. yee, C.H. Arrowsmith, V.Y. Orekhov, J. Biomol. NMR 33 (2005) 1–14.
[34] K. Kazimierczuk, A. Zawadzka, W. Kozminski, I. Zhukov, J. Biomol. NMR 36 (2006) 157–168.
[35] J.-B. Poullet, D.M. Sima, S. van Huffel, J. Magn. Reson. 195 (2008) 134–144.
[36] P. Bendel, J. Magn. Reson. 86 (1990) 509–515.
[37] K.E. Washburn, C.D. Eccles, P.T. Callaghan, J. Magn. Reson. 194 (2008) 33–40.
[38] A. Guillermot, J.-P. Cohen Addad, D. Bytchenkoff, J. Chem. Phys. 113 (2000) 5098–5106.
[39] R.L. Kleinberg, A. Sezginer, D.D. Griffin, J. Magn. Reson. 97 (1992) 466–485.
[40] G. Eidmann, R. Savelsberg, P. Blümler, B. Blümich, J. Magn. Reson. A 122 (1996) 104–109.
[41] P.S. Aptaker, P.J. McDonald, J. Mitchell, Magn. Reson. Imaging 25 (2007) 548.
[42] M.D. Hürlimann, Magn. Reson. Imaging 19 (2001) 375–378.
[43] S. Bobroff, G. Guillot, C. Riviere, L. Cuiec, J.C. Roussel, Magn. Reson. Imaging 14 (1996) 907–909.
[44] M.D. Hürlimann, J. Magn. Reson. 131 (1998) 232–240.
[45] P.J. Prado, B.J. Balcom, S.D. Beyea, R.L. Armstrong, T.W. Bremner, P.E. Grattan-Bellew, Magn. Reson. Imaging 16 (1998) 521–523.
[46] S. Rodts, D. Bytchenkoff, T. Fen-Chong, J. Magn. Reson. 204 (2010) 64–75.
[47] H.G. Feichtinger, K. Gröchenig, Theory and practice of irregular sampling, in: J.J. Benedetto, M.W. Frazier (Eds.), Wavelets: Mathematics and Applications, CRC Press, London, 1993, pp. 305–363.
[48] A. Aldroubi, K. Gröchenig, SIAM Rev. 43 (2001) 585–620.
[49] H.G. Feichtinger, K. Gröchenig, T. Strohmer, Numer. Math. 69 (1995) 423–440.
[50] V.A. Kotelnikov, On the Transmission Capacity of 'Ether' Wire in Electro-Communication, Material for the First All-Union Conference on Questions of Communication, Izd. Red. Upr. Svyazzi RKKA, Moscow, 1933.
[51] C.E. Shannon, Bell Labs Tech. J. 27 (1948) 379–423. and 623–656.
[52] R.J. Marks II, Introduction to Shannon Sampling and Interpolation Theory, Springer-Verlag, New York, 1991.
[53] L. Reichel, G.S. Ammar, W.B. Gragg, Math. Comput. 57 (1991) 273–289.
[54] T. Strohmer, R. Vershynin, J. Fourier Anal. Appl. 15 (2009) 262–278.
[55] J. Idier, (sous la direction) Approche bayésienne pour les problèmes inverses, Hermès Science Publications, Paris, 2001.
[56] G.L. Bretthorst, J. Magn. Reson. 88 (1990) 533–551.
[57] W.H. Press, S.A. Teukolsky, W.T. Vetterling, B.P. Flannery, Numerical Recipes in Fortran: The Art of Scientific Computing, Cambridge University Press, New York, 1986.
[58] G. Zhu, A. Bax, J. Magn. Reson. 90 (1990) 405–410.
[59] A. Dutt, V. Rokhlin, Appl. Comput. Harmon. Anal. 2 (1995) 85–100.